

Stimulated Emission and Lasing from CdSe/CdS/ZnS Core-Multi-Shell Quantum Dots by Simultaneous Three-Photon Absorption

Yue Wang, Van Duong Ta, Yuan Gao, Ting Chao He, Rui Chen, Evren Mutlugun, Hilmi Volkan Demir,* and Han Dong Sun*

Due to the quantum confinement effect, colloidal semiconductor quantum dots (QDs) exhibit various advantageous properties as optical gain media including emission wavelength tunability over a wide spectral range through simply tailoring the size of QDs, potentially low lasing threshold and temperature-insensitive lasing performance.^[1–4] However, the achievement of stimulated emission (SE) and lasing from QDs is unexpectedly challenging since the excited carriers suffer from Auger recombination (AR) and trapping by surface defects.^[5–9] With the advent of high-quality colloidal QDs, the issue of surface trapping has been somehow addressed. Subsequently, Klimov et al. first observed SE from CdSe QDs, and demonstrated that the radiative recombination of excitons in QDs was rapid enough to compete against nonradiative AR.^[1] Since then, SE and lasing action have been extensively demonstrated in various kinds of colloidal semiconductor QDs mainly based on one-photon pumping using UV-excitation wavelengths.^[2,6,10–13]

However, due to the poor spatial resolution based on one-photon pumping, it would be very difficult to pump merely the gain material without excitation of undesired parts.^[14] In addition, as the surface of a myriad of gain media can be easily contaminated, the lasing performance under one-photon excitation would be drastically affected.^[15] In contrast, multi-photon pumping possesses a longer excitation wavelength in infrared

(IR) range and a nonlinear dependence of absorption on excitation intensity,^[16] thus leading to a larger penetration depth into samples and a higher spatial resolution. The employment of two-photon pumping has indeed, to some extent, mitigated the above limitations.^[15] Naturally, even a higher-order nonlinear pumping based on three-photon absorption (3PA) should be adopted in order to further circumvent these issues.^[17] Notably, in the field of biophotonics, long excitation wavelengths and high-order nonlinear absorption are strongly preferred.^[18] Although the utilization of two-photon excitation has extended the penetration depth into tissues up to several hundreds of micrometers, as limited by the strong tissue scattering,^[19] an even larger depth of up to a few millimeters is desperately needed to satisfy the growing demand for biological research and applications,^[18–20] which can be efficiently realized by using three-photon pumping.^[17–19]

Three-photon excited SE from organic dyes in solution has been demonstrated by He et al.^[16] However, the intrinsic poor stability of organic dyes makes them too difficult to achieve three-photon pumped SE in solid state, thus limiting their practical applications. Unfortunately, because of the much smaller multi-photon absorption cross-sections compared to one-photon counterparts and a lack of adequately robust QDs to withstand the inevitably high intensity under multi-photon excitation,^[14,21] only a limited number of studies have reported the two-photon pumped SE and lasing action from colloidal semiconductor QDs.^[21–23] Nevertheless, to date, three-photon induced SE or lasing action from semiconductor QDs, which could offer new enabling tools in biology and photonics as well as in their intersection of biophotonics, has not yet been demonstrated.

Herein, we engineer CdSe/CdS/ZnS core-multi-shell QDs forming quasi-type-II band alignment in an attempt to both enhance the 3PA cross-sections and suppress nonradiative AR. In this work, three-photon induced SE and coherent random lasing from close-packed solids of these QDs are achieved for the first time. The physical mechanisms are clearly elucidated in terms of enhanced 3PA cross-sections, suppression of AR and reduced reabsorption effect. Our results validate the feasibility of colloidal CdSe/CdS/ZnS QDs as optical gain media based on three-photon pumping and could also offer new possibilities in biophotonics where long excitation wavelengths and high-order nonlinear excitation are strongly desired, including laser-assisted disease diagnostics and deep tissue sensing.

It is known that the ideal shell passivating CdSe-cores should have both small lattice mismatch and large band offsets with respect to those of CdSe-cores.^[24,25] Although CdS-shells have

Y. Wang, V. D. Ta, Y. Gao, Dr. T. C. He,
Dr. R. Chen, Prof. H. D. Sun
Division of Physics and Applied Physics
School of Physical and Mathematical Sciences
Nanyang Technological University
Singapore 637371, Singapore
E-mail: HDSun@ntu.edu.sg



Dr. E. Mutlugun, Prof. H. V. Demir
School of Electrical and Electronic Engineering
Luminous! Center of Excellence for Semiconductor Lighting and Displays
Nanyang Technological University
Nanyang Avenue, Singapore 639798, Singapore
E-mail: HVDemir@ntu.edu.sg

Prof. H. V. Demir, Prof. H. D. Sun
Centre for Disruptive Photonic Technologies (CDPT)
Nanyang Technological University
Singapore, Singapore 637371, Singapore

Prof. H. V. Demir
Department of Electrical and Electronics Engineering
Department of Physics, and UNAM-National Nanotechnology
Research Center
Bilkent University
Bilkent, Ankara

DOI: 10.1002/adma.201305125

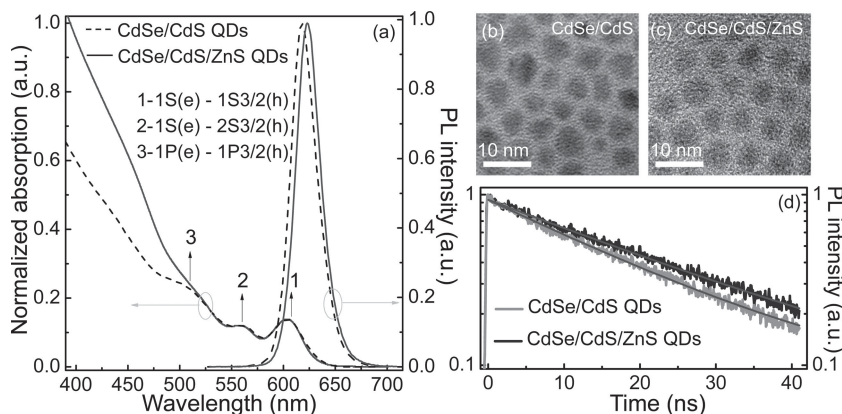


Figure 1. a) Normalized UV-visible absorption spectra and normalized PL spectra of CdSe/CdS and CdSe/CdS/ZnS QDs excited at 441 nm using a continuous He-Cd laser. The arrows mark the positions of the three well-resolved excitonic transitions. b) The TEM image of CdSe/CdS QDs. c) The TEM image of multi-shell coated CdSe/CdS/ZnS QDs. d) PL decay dynamics of dilute solutions of CdSe/CdS and CdSe/CdS/ZnS QDs with low excitation intensity ($\langle N \rangle = 0.05$) at wavelength of 400 nm.

similar lattice parameters, the low band offsets impede the electronic passivation.^[24] As a result, additional ZnS-shells with much larger band offsets are grown in order to fully passivate CdSe-cores in this work. **Figure 1a** presents the linear UV-visible absorption and one-photon excited photoluminescence (PL) of CdSe/CdS QDs and CdSe/CdS/ZnS core-multi-shell QDs dispersed in toluene at room temperature. It is important to note that the CdS layers in CdSe/CdS/ZnS QDs are thicker than those in CdSe/CdS QDs based on the fabrication process (see Experimental Section), and the extra absorption at higher energy starting from ~ 500 nm of CdSe/CdS/ZnS QDs with respect to that of CdSe/CdS QDs just arises from the thicker CdS layers in CdSe/CdS/ZnS QDs.^[6,10] It is found that the lowest three exciton transitions ($1S(e)-1S_{3/2}(h)$, $1S(e)-2S_{3/2}(h)$ and $1P(e)-1P_{3/2}(h)$)^[5] are well resolved, which, together with the narrow emission linewidth (~ 30 nm), implies the high quality of our samples. It is known that the lifetime of QDs changes with the average number of excitons per QD $\langle N \rangle$ following excitation.^[10] Therefore, the lifetimes of CdSe/CdS and CdSe/CdS/ZnS QDs with the same $\langle N \rangle = 0.05$ after photoexcitation rather than intensity are presented (excitation wavelength: 400 nm) (Figure 1d). Detailed calculation of $\langle N \rangle$ can be found in the Supporting Information. In order to avoid interactions between QDs, dilute solutions of CdSe/CdS and CdSe/CdS/ZnS QDs (2.6×10^{18} QDs/L and 2.3×10^{18} QDs/L for CdSe/CdS and CdSe/CdS/ZnS QDs, respectively) are used for this characterization. The PL decay curves monitored at peak wavelength can be well-fitted by a single-exponential-decay function with lifetimes of 19.5 ns and 25.6 ns for CdSe/CdS and CdSe/CdS/ZnS QDs, respectively. The prolonged lifetime after multi-shell coating are mostly due to the increased leakage of electrons into the thick CdS-shells in CdSe/CdS/ZnS QDs as a result of the small conduction-band offset,^[26] thus reducing the overlap between electron and hole wave functions, which is also evident from the observable redshift of the emission peak wavelength following multi-shell coating (Figure 1a). According to the transmission electron microscopy (TEM) images (Figure 1b and 1c) and the TEM statistical information on

size distribution (Figure S1a and S1b), the sizes of CdSe/CdS and CdSe/CdS/ZnS QDs are estimated to be 4.96 ± 0.32 nm and 6.57 ± 0.63 nm, respectively.

The main reasons for the absence of three-photon pumped SE or lasing from colloidal semiconductor QDs are the extremely small 3PA cross-sections of common QDs and a lack of robust QDs to withstand the inevitably high power excitation.^[14,21] Importantly, it has been firmly revealed that the two-photon absorption (2PA) cross-sections can be remarkably influenced by shell constituent and shell thickness in various semiconductor QDs contributing to several physical effects,^[27–30] which prompts us to explore the 3PA property of CdSe-based QDs by modifying the shells covering the CdSe-cores since there are similarities among multi-photon absorption processes.^[17] We found that the 3PA cross-sections of CdSe/CdS QDs were

largely enhanced after coating with thicker CdS-shells and ZnS-shells, as will be elaborated in the following part. It is worth noting that the chemical- and photo-stability could be greatly improved by covering with thicker CdS-shells and ZnS-shells since the cores can be well-protected and isolated from external environment.^[10,24,31] Therefore, the main impediments for achieving three-photon pumped SE and lasing from colloidal QDs can be simultaneously addressed by using CdSe/CdS/ZnS core-multi-shell QDs.

The 3PA properties of the samples were carefully investigated by using open-aperture Z-scan technique^[32] with femtosecond laser pulses at 1300 nm. Before characterization of the samples, the validity of the Z-scan system is calibrated using CS₂ liquid as a reference.^[20,33] The third-order nonlinear refractive index was determined to be 3.2×10^{-6} cm²/GW, which agrees well with the previously measured value (3.3×10^{-6} cm²/GW) under similar conditions.^[20,33] For the Z-scan measurements, CdSe/CdS and CdSe/CdS/ZnS QDs were dispersed in toluene at exceptionally high concentrations (2.6×10^{20} QDs/L and 2.3×10^{20} QDs/L for CdSe/CdS and CdSe/CdS/ZnS QDs, respectively) and injected into 1 mm thick quartz cuvettes, which moved along the laser beam propagation axis. The linear transmittances of the samples at 1300 nm are nearly unity, which reflects the good solubility of these QDs.^[32,33] **Figure 2a** displays the open-aperture Z-scan curves of CdSe/CdS QDs, CdSe/CdS/ZnS QDs and pure toluene at intensity of 100 GW/cm². The flat response curve of toluene indicates that the nonlinear absorption of the solvent is negligible and the nonlinear absorption signals entirely stem from CdSe/CdS and CdSe/CdS/ZnS QDs. The normalized transmittance of the samples can be well-fitted with the theoretical analysis for 3PA according to Z-scan theory^[34] as given by:

$$T = \pi^{-1/2} p_0^{-1} \exp(-\alpha_0 L) \times \int_{-\infty}^{\infty} \ln \left\{ \left[1 + p_0^2 \exp(-2x^2) \right]^{1/2} + p_0 \exp(-x^2) \right\} dx$$

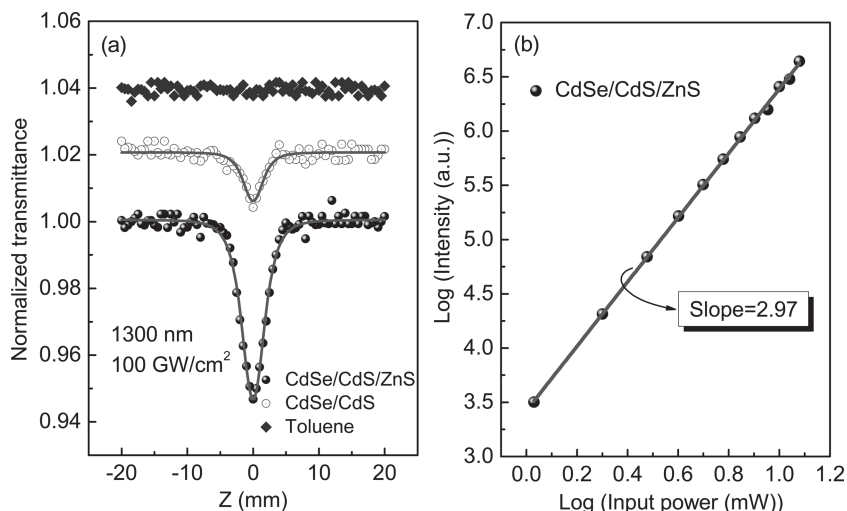


Figure 2. a) Open-aperture Z-scan curves of solvent, CdSe/CdS and CdSe/CdS/ZnS QDs at a wavelength of 1300 nm and incident intensity of 100 GW cm^{-2} . The solid lines are the fitting curves based on Z-scan theory. b) Log-log plots of the PL intensities of CdSe/CdS/ZnS QDs as a function of the excitation power at 1300 nm. The red line is the linear fitting with a slope of 2.97.

where $p_0 = (2\gamma I_0^2 L_{\text{eff}})^{1/2}$, $L_{\text{eff}} = (2\alpha_0)^{-1} [1 - \exp(-2\alpha_0 L)]$, I_0 is the incident intensity along the laser beam axis, $L = 1 \text{ mm}$ is the optical path length through the sample, and α_0 and γ are the linear and 3PA coefficients, respectively. Finally, the 3PA cross-sections are extracted to be 4.3×10^{-78} and $2.8 \times 10^{-77} \text{ cm}^6 \text{ s}^2 \text{ photon}^{-2}$ for CdSe/CdS and CdSe/CdS/ZnS QDs, respectively. For comparison, our results and other data taken from the literature are summarized in Table S1 (see Supporting Information). It is found that the 3PA cross-sections of CdSe/CdS/ZnS QDs are nearly one order of magnitude larger than those of commonly used II-VI QDs and four orders larger than that of Rhodamine 6G.^[35–37] The large 3PA cross-sections after multi-shell coating can be attributed to an antenna-like effect where the thick CdS shell efficiently absorbs photons and rapidly funnels the photocarriers into CdSe core within $\sim 1 \text{ ps}$,^[10,30] the photoinduced screening of the internal field stemming from the lattice mismatch between CdSe core and CdS/ZnS shells^[27,28] and the local field effect.^[27,29] In order to further confirm the 3PA and emission process, power dependent up-conversion PL was performed. Figure 2b depicts the log-log plots of PL intensities of CdSe/CdS/ZnS QDs solution as a function of the input power at 1300 nm. The nearly cubic power dependence of the PL signals unambiguously verifies the 3PA and emission process.^[17]

To exploit the enhanced 3PA properties and robustness of CdSe/CdS/ZnS core-multi-shell QDs, SE from these QDs was investigated using stripe pumping configuration (Figure 3c). The thin film of colloidal CdSe/CdS/ZnS QDs was prepared by drop-casting high concentration QDs solution onto hydrophobic glass slides at room temperature. It is found that QDs solution can spread very well on the glass slides and optically smooth surfaces are formed as shown from the large-scale optical microscopy image ($100 \mu\text{m} \times 100 \mu\text{m}$) (Figure S2a) and small area atomic force microscopy (AFM) image ($5 \mu\text{m} \times 5 \mu\text{m}$) (Figure 3b). The root-mean-square and peak-to-peak surface roughness are 1.8 nm and 20.2 nm, respectively, which are far

smaller than excitation and emission wavelengths. We do note that sometimes well-defined cracks are formed (Figure S2b) possibly by tensile stress in the plane of the film during solvent evaporation.^[2] The packing density is estimated to be $\sim 30\%$ according to the film thickness of $\sim 5 \mu\text{m}$ (Figure S2c) and the corresponding first exciton absorbance (Figure 4a).^[22,38] Figure 3a depicts the evolution of three-photon excited PL spectra with progressively higher pump intensities at 1300 nm. Below the pump threshold, only spontaneous emission with a full width at half-maximum (FWHM) of $\sim 30 \text{ nm}$ was detected, while a narrower peak with FWHM of $\sim 8 \text{ nm}$ emerged above the threshold corresponding to SE. The dependence of integrated PL intensity on pump intensity is given in the inset of Figure 3a. This characterization shows a three-stage process as the pump intensity increases. Below the pump intensity of $\sim 9.0 \text{ mJ cm}^{-2}$, the PL signals present a nearly cubic dependence of the pump intensity, which agrees with the 3PA and emission process. Thereafter, it undergoes saturation mainly due to the effect of fast AR near multi-exciton regime. Finally, an abruptly sharp increase of the integrated PL intensities indicates the development of SE with a threshold of 14.5 mJ cm^{-2} . The optical images below and above the threshold are shown in the insets (1) and (2), respectively, in Figure 3a. The appearance of a bright spot above the threshold is a direct evidence of SE.^[2] Notably, the peak of SE is blue-shifted with regard to its corresponding spontaneous emission maximum, in stark contrast to type-I QDs, which typically show redshift for the SE peak.^[22,23,39] This blueshift is an indicative of repulsive exciton-exciton interactions owing to the imbalance of spatial distribution of positive and negative charges in CdSe/CdS/ZnS QDs with quasi-type-II band alignment (Figure 3d),^[10,39] in which the holes are completely confined in the CdSe core, while the electrons spread over both the CdSe core and the CdS shell.^[6] Correspondingly, the overlap of electron-hole wave functions remarkably decreases while those for electron-electron and hole-hole greatly increase as illustrated with the dashed ellipse lines. Eventually, the attractive exciton-exciton interactions in type-I QDs transform into repulsive counterparts in these quasi-type-II CdSe/CdS/ZnS QDs. The exciton-exciton interaction energy (Δ_{XX}) is estimated to be $\sim 22 \text{ meV}$ according to $\Delta_{XX} = \hbar\omega_{XX} - \hbar\omega$, where $\hbar\omega_{XX}$ is the photon energy produced by radiative biexciton recombination and $\hbar\omega$ is the single exciton energy.^[39] Noticeably, such quasi-type-II configuration can be very favorable as gain media in view of AR suppression.^[6] It has been demonstrated that the rate of AR in QDs mainly depends on the degree of spatial overlap between electron and hole wave functions involved in AR, exciton-exciton interactions and the profile of interface potential.^[10] The spatial separation between electrons and holes in CdSe/CdS/ZnS QDs will decrease the electron-hole overlapping, thereby reducing AR.^[39] It is worth mentioning that the interdiffusion of atoms within different shells is unavoidable during the one-pot fabrication,^[26,31] as

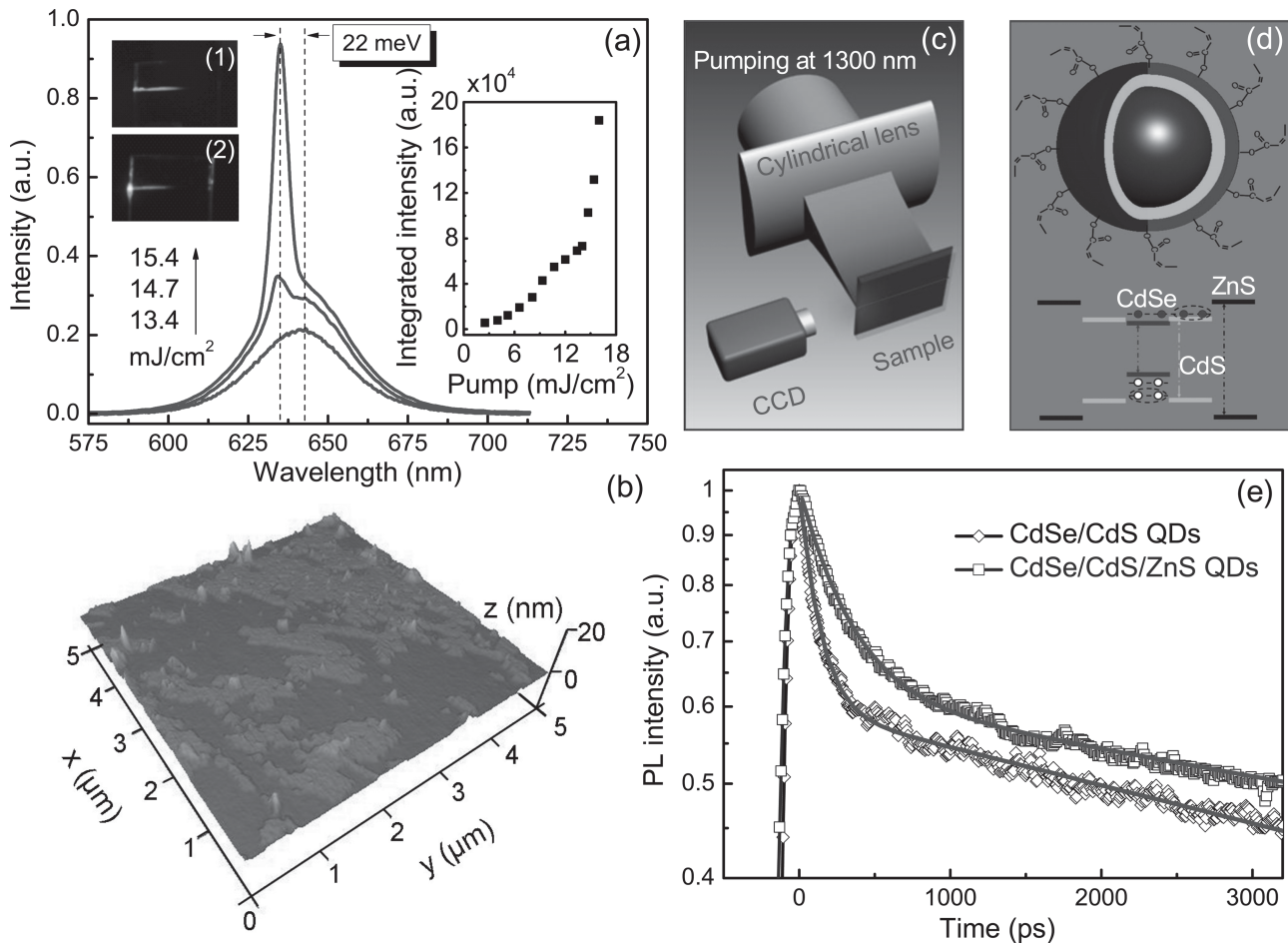


Figure 3. a) Achievement of SE from close-packed CdSe/CdS/ZnS core-multi-shell QDs film as the pumping intensity increases at 1300 nm. The inset on the right shows the integrated PL intensity with respect to the pump intensity. The insets (1) and (2) on the left show the optical images below and above the threshold, respectively. b) AFM image of close-packed CdSe/CdS/ZnS QDs film under tapping mode. c) Stripe pumping configuration and collection from the edge of our sample. d) Schematic of the structure of CdSe/CdS/ZnS core-multi-shell QDs and the corresponding energy band alignments. e) PL decay dynamics at pumping intensity just below SE threshold of CdSe/CdS/ZnS QDs and that of CdSe/CdS QDs with the same $\langle N \rangle = 1.05$ after photoexcitation.

a result, a smooth interface potential rather than a sharp one is expected, which could further mitigate AR since such loose potential profile will limit AR with more strict momentum conservations compared to steep interface potential.^[40] Time-resolved PL measurements were adopted to study the excitonic dynamics in CdSe/CdS/ZnS QDs solids under three-photon pumping.^[5] At low intensity (5.4 mJ cm^{-2} or $\langle N \rangle = 0.06$), the PL dynamic curve can be well-fitted by single-exponential decay function with lifetime of 16.5 ns (Figure S3a). When the intensity increases to just below the SE threshold (14.0 mJ cm^{-2} , corresponding to $\langle N \rangle = 1.05$), the PL decay curve taken at peak position can be well fitted by a two-exponential-decay function (Figure 3e). Specifically, the lifetime of the fast decay component, corresponding to AR,^[5,10] is resolved to be ~ 310 ps. In contrast, the AR lifetime of CdSe/CdS QDs with $\langle N \rangle = 1.05$ is only ~ 130 ps, which clearly confirms the suppression of AR in CdSe/CdS/ZnS QDs. The slower lifetime component, corresponding to single-exciton decay, is derived to be 15.1 ns, similar to the value measured at low excitation intensity ($\langle N \rangle =$

0.06). Furthermore, it is known that exciton distribution in QDs follows the Poisson statistics: $P(n) = \frac{\langle N \rangle^n e^{-\langle N \rangle}}{n!}$,^[2,39] where n is the number of excitons per QD. The amplitude ratio of fast AR to slow single-exciton decay lifetime components can be extracted from the two-exponential-decay fitting to be 0.44, where the AR and single-exciton decay are contributed by subsets of QDs with $n > 1$ and $n > 0$, respectively. Therefore, the average number of excitons per QD $\langle N \rangle$ is derived to be 1.07, which agrees with the value ($\langle N \rangle = 1.05$) calculated from 3PA cross-sections obtained through Z-scan characterization. As the pumping intensity well exceeds the threshold, the ultrafast SE obviously dominates over AR with much shorter lifetime whose measurement is limited by the temporal resolution (~ 50 ps) of our streak camera system. The evolution of PL dynamics with varied pumping intensities can be clearly seen from the spectrograms shown in Figure S3b–d.

In order to comprehensively investigate three-photon pumped SE, the one- (at 480 nm) and two-photon (at 800 nm) pumped SE are comparatively studied. Figure 4a illustrates

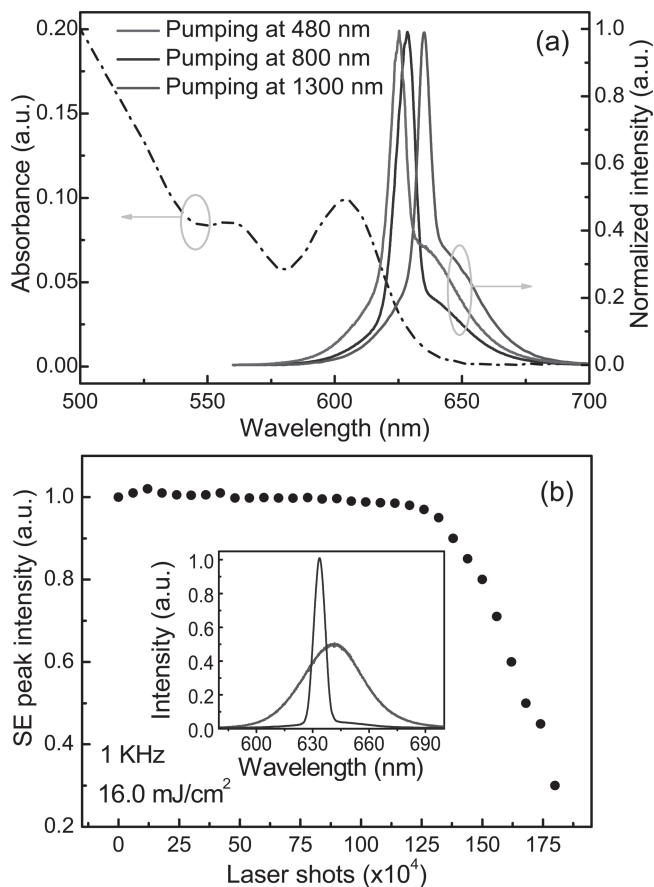


Figure 4. a) Absorbance of close-packed CdSe/CdS/ZnS QDs film and normalized SE spectra under one-, two- and three-photon pumping at intensities of 0.8, 8.5 and 15.4 mJ cm^{-2} , respectively. b) SE peak intensity from CdSe/CdS/ZnS QDs film at intensity of 16.0 mJ cm^{-2} based on three-photon pumping as a function of laser shots. The inset shows the SE spectrum at intensity of 16.0 mJ cm^{-2} and spontaneous emission spectrum below the threshold (multiplied by 50 times).

the spectra of SE pumped at 480 nm, 800 nm and 1300 nm at intensities of 0.8, 8.5 and 15.4 mJ cm^{-2} , respectively. A summary of parameters for one-, two- and three-photon pumped SE are listed in Table 1. It is found that the SE peaks pumped at 800 nm and 1300 nm are progressively red-shifted with respect to that at 480 nm. Noticeably, Kambhampati et al. also observed redshift of SE peaks in CdSe QDs when pumping at higher excitonic states and was attributed to multiexciton interactions.^[41,42] However, the spontaneous emission peaks in

Table 1. A summary of SE parameters based on one-, two- and three-photon pumping.

	Excitation wavelength [nm]	SE peak wavelength [nm]	Δ_{xx} [meV]	Threshold [mJ cm^{-2}]	Average excitons per QD at SE threshold
1-photon	480	625	23	0.6	1.9
2-photon	800	628	23	8.2	1.5
3-photon	1300	635	22	14.5	1.2

this work (Figure 4a) also red-shift accordingly as higher-order nonlinear excitation was used, which is different from those by state-resolved pumping.^[41] In our case, the gradual redshift of the SE peaks can be mostly attributed to the increased contribution to PL intensity from the subset of slightly larger particles,^[14] which show luminescence in lower energy part since multi-photon absorption cross-sections of QDs are revealed to increase with size and show power-law dependence of ~ 4 to their diameters due to the increased density of states (DOS) of larger dots.^[29,30] Fortunately, this redshift of the SE peaks can reduce reabsorption effect as seen from Figure 4a, which should be responsible for the successive decrease of the calculated average number of excitons per QD $\langle N \rangle$ at the threshold based on one- ($\langle N \rangle = 1.9$), two- ($N = 1.5$) and three-photon pumping ($N = 1.2$) (see Table 1).^[22]

To test the stability of this system, the variation of SE peak intensity was recorded as a function of the number of pumping pulses with a pulse-width of 100 fs and a repetition rate of 1 KHz (Figure 4b). The pumping intensity of 16 mJ cm^{-2} is chosen to ensure that the emission spectrum is dominated by SE rather than spontaneous emission (Figure 4b, inset). Thanks to the super chemical- and photo-stability of CdSe/CdS/ZnS QDs, the system can keep 90% of its initial SE maximum over as many as $\sim 1.2 \times 10^6$ shots, which validates the viability of CdSe/CdS/ZnS QDs as optical gain material based on three-photon pumping.^[21,22]

Recently, random lasers have attracted great attention thanks to their low cost and easy fabrication without the need for additional cavities and offering a wide range of potential applications.^[43,44] The dominating challenges to achieve random lasing lie in the realization of high optical gain and strong scattering simultaneously.^[44,45] In this work, the self-assembled clusters of CdSe/CdS/ZnS QDs are used as the optical gain media as well as the strong scattering centers taking advantage of the high refractive index of semiconductor QDs. Specifically, the CdSe/CdS/ZnS QDs film with rich self-assembled clusters was obtained by drying the QDs suspension drop-casted onto glass slides at a relatively high temperature (50 ~ 60 °C) in an oven. The surface morphology was investigated through large-scale optical microscopy image (100 $\mu\text{m} \times 100 \mu\text{m}$) (Figure S2d) and small-area AFM image (5 $\mu\text{m} \times 5 \mu\text{m}$) (Figure 5b). Different from the film made at room temperature, a pretty rough surface of CdSe/CdS/ZnS QDs film with a root-mean-square roughness of 29.5 nm and a peak-to-peak surface roughness of 189.2 nm was obtained due to faster solvent evaporation. For the lasing action investigation, a similar pumping configuration was employed as used in SE characterization. The PL spectra pumping at 1300 nm with different intensities are given in Figure 5a. We can see that at relatively low excitation intensities ($< 17.1 \text{ mJ cm}^{-2}$), the PL spectra are dominated by broad spontaneous emission with a FWHM of ~ 30 nm. When the pumping intensities keep increasing, narrow discrete spikes with a linewidth of ~ 0.4 nm emerge and superimpose on the corresponding SE peaks. More and more spikes turn up at higher excitation intensity. The spectrally integrated intensities from 632 to 642 nm with respect to pumping intensity are presented in the inset of Figure 5a. The abrupt increase of the integrated intensity indicates the achievement of random lasing with a threshold of 17.1 mJ cm^{-2} . It is known that random

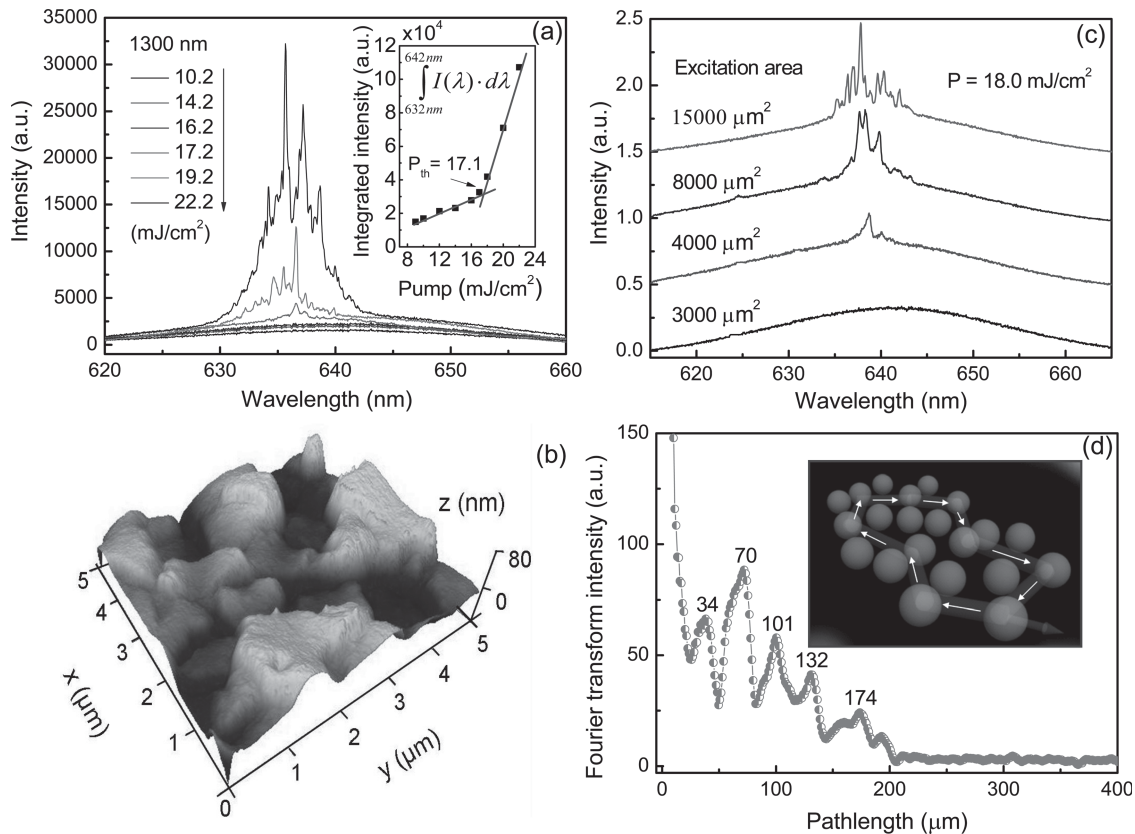


Figure 5. a) Development of coherent random lasing from self-assembled CdSe/CdS/ZnS QD solids as the pumping intensity increases. The inset shows the integrated PL intensity (632–642 nm) as a function of the pump intensity. b) AFM image of self-assembled CdSe/CdS/ZnS QD solids under tapping mode. c) Lasing spectra of the sample with different excitation areas at the intensity of 18.0 mJ cm⁻². d) Fourier transform of the lasing spectrum with the excitation intensity of 19.2 mJ cm⁻². The inset illustrates the schematic of fundamental cavity, where the spheres denote the QDs clusters.

lasing can be mainly classified into two categories on the basis of different feedback mechanisms: incoherent random lasing and coherent random lasing.^[44,46] For incoherent random lasing, there is only intensity or energy feedback. Therefore, it is wavelength insensitive and normally occurs in disordered active systems with weak scattering strength. The spectral shape of incoherent random lasing is featured by a narrowing peak at the gain maximum with a linewidth of several nanometers, which can be regarded as reinforced SE with enlarged optical path due to scattering.^[44] In contrast, the feedback for coherent random lasing is provided by field or amplitude mechanism, where closed optical loops would be formed thanks to the interference of multiple scattering and serve as ring cavities.^[47] As a result, discrete super-narrow peaks or spikes with a linewidth of usually less than 1 nm will appear and superimpose on the SE band.^[44,46,48] Based on the characteristics of the lasing performance from our sample, we attribute the lasing action from the self-assembled CdSe/CdS/ZnS QDs clusters to coherent random lasing.^[46,49] Due to different loss of these random ring cavities, the threshold for the lasing action in individual cavity is different.^[45] Under higher pumping intensities, more ring cavities can meet the threshold requirements, and thus more spikes turn up, which is consistent with our results. Besides, the pumping area dependent

random lasing action was performed in order to further confirm the coherent random lasing mechanism.^[44,45] According to the coherent random lasing theory, there is a critical area for the formation of ring cavities.^[45] When the pumping area is below this value, there is not enough space for the formation of closed loops. As the excitation area keeps increasing, more and more closed loops can find sufficient space to develop in the disordered system, accompanied by more and more spikes appearing in the emission spectra.^[45,48,50] Figure 5c shows the evolution of PL spectra of our sample with increasing pumping stripe length, and hence the excitation area at a constant intensity of 18.0 mJ cm⁻². It is found that no lasing action occur with small excitation area (<4000 μm²), while more and more spikes emerge with increasing the pumping area, which again validates the coherent random lasing mechanism. In order to derive the cavity length of the random lasing action from the sample, power Fourier transform (FT)^[47,51] of the emission spectrum was utilized. Figure 5d illustrates the FT-processed spectrum at the excitation intensity of 19.2 mJ cm⁻². The cavity length, or effective perimeter of the closed loops, L , is given by: $L = 2\pi d/n$, where d is an optical path length parameter whose value is determined by the peak positions in FT spectrum and n is the refractive index of the gain material.^[47,51] From the figure we can see that the FT spectrum shows a series of

peaks at positions of 34, 70, 101, 132 and 174 μm . Since the separations between neighboring peaks are quite similar, we attribute the peak at 34 μm to the fundamental cavity length,^[52] while the subsequent peaks at 70, 101, 132 and 174 μm arise from the light traveling multiple trips around the fundamental cavity.^[47,51,52] The inset in Figure 5d illustrates the fundamental cavity formed in this disordered system as a result of strong scattering. The fundamental cavity length is estimated to be $L \approx 126 \mu\text{m}$, taking $d = 34 \mu\text{m}$ and $n = 1.7$ in our sample.^[2] It should be noted that the critical area determined in pumping area dependent measurements is about 2.5 times larger than the area ($\sim 1610 \mu\text{m}^2$) of the fundamental cavity calculated from fundamental cavity length, which can be attributed to the different geometry and randomness of closed loops.^[45,50]

In conclusion, in order to overcome the main challenges for achieving direct three-photon pumped SE and lasing action from colloidal semiconductor QDs, we adopted the robust CdSe/CdS/ZnS core-multi-shell QDs as the optical gain media. The 3PA cross-sections of CdSe/CdS/ZnS QDs are determined to be as high as $2.8 \times 10^{-77} \text{ cm}^6 \text{ s}^2 \text{ photon}^{-2}$. Thanks to the quasi-type-II band alignment in CdSe/CdS/ZnS QDs, the AR has been to some extent suppressed. Moreover, through comparative investigation of one-, two- and three-photon pumped SE from CdSe/CdS/ZnS QDs, we found that reabsorption effect was relatively reduced under three-photon pumping. Eventually, three-photon induced SE and coherent random lasing from close-packed solids of colloidal semiconductor QDs have, for the first time, been demonstrated. Our results indicate that CdSe/CdS/ZnS core-multi-shell QDs can be reliable frequency up-converting optical gain media and could hold great promise for biomedical and biological applications including laser-assisted diagnostics and therapy.

Experimental Section

Synthesis of Colloidal Semiconductor Quantum Dots: Previously reported facile one-pot method^[31,53] was adopted to fabricate CdSe/CdS/ZnS QDs. In brief, cadmium oxide (CdO, 1 mmol), OA (18.85 mmol) and zinc acetate ($\text{Zn}(\text{acet})_2$, 2 mmol) were mixed with 25 mL 1-octadecene (1-ODE) in a flask. Then, the mixture was evacuated for 15 min and heated to 300 °C under nitrogen condition. After that, selenium (Se) precursor made by dissolving Se power (0.2 mmol) in trioctylphosphine (TOP, 0.2 mmol) was quickly added into the reaction flask at 300 °C. After 3 min, 0.3 mL dodecanethiol (DT) was injected slowly into the mixture. The reaction lasted for 20 min in order to obtain CdSe/CdS QDs. Subsequently, sulfur (S) precursor made by dissolving S power (2 mmol) in TOP (1 mmol) was added to react with the excess Cd ions and passivate the surface with ZnS shell. Finally, the QDs were purified with methanol for several times and dissolved in toluene solvent.

Characterization: A femtosecond amplified-pulsed laser system was used as the laser source. The output wavelength can be continuously tuned from 250 nm to 2.6 μm through an optical parameter amplifier. The pulse-width and repetition rate are 100 fs and 1 KHz, respectively. The schematic of Z-scan experimental setup is shown in Figure S4. The laser beam was separated into two parts through a beam splitter. The reflected beam was recorded (Detector 1) in order to reduce the influence of pulse fluctuations. The transmitted beam was focused onto a 1 mm thick quartz cuvette containing the samples with radius of $\sim 20 \mu\text{m}$ by a circular lens with a focus length of 20 cm, which moved along the laser beam axis, and finally detected by a Ge biased detector (Detector 2) using standard lock-in amplifier technique.

For the three-photon pumped SE, coherent random lasing and time-resolved PL measurements, the same laser system as used in Z-scan characterization was adopted as the excitation source. The excitation beam at a wavelength of 1300 nm was focused onto the sample with dimensions of $100 \mu\text{m} \times 10 \text{ mm}$ through a cylindrical lens with a focus length of 75 mm. For the three-photon pumped SE and coherent random lasing experiments, the PL signals from the edge of the sample was dispersed by a 3/4 m monochromator assisted with a pair of collection lenses and a short-pass filter (cut-off wavelength: 700 nm) and recorded by a silicon charged coupled device (CCD) with a spectral resolution of $\sim 0.05 \text{ nm}$. For the time resolved PL measurements, the PL signals were detected by an Optronics streak camera system with time resolution of $\sim 50 \text{ ps}$.

Supporting Information

Supporting Information is available from the Wiley Online Library or from the author.

Acknowledgements

This work is supported by the Singapore Ministry of Education through the Academic Research Fund under Projects MOE 2011-T3-1-005 (Tier 3) and RG63/10 (Tier 1) and from the Singapore National Research Foundation through the Competitive Research Programme (CRP) under Projects No. NRF-CRP6-2010-02 and NRF-CRP5-2009-04).

Received: October 15, 2013

Revised: November 25, 2013

Published online: February 6, 2014

- [1] V. I. Klimov, A. A. Mikhailovsky, S. Xu, A. Malko, J. A. Hollingsworth, C. A. Leatherdale, H. J. Eisler, M. G. Bawendi, *Science* **2000**, *290*, 314.
- [2] C. Dang, J. Lee, C. Breen, J. S. Steckel, S. Coe-Sullivan, A. Nurmikko, *Nat. Nanotechnol.* **2012**, *7*, 335.
- [3] B. Guzelturk, P. L. H. Martinez, Q. Zhang, Q. Xiong, H. Sun, X. W. Sun, A. O. Govorov, H. V. Demir, *Laser Photonics Rev.* **2013**, DOI: 10.1002/lpor.201300024.
- [4] P. Kambhampati, *J. Phys. Chem. Lett.* **2012**, *3*, 1182.
- [5] V. I. Klimov, *Annu. Rev. Phys. Chem.* **2007**, *58*, 635.
- [6] M. Zavelani-Rossi, M. G. Lupo, R. Krahne, L. Manna, G. Lanzani, *Nanoscale* **2010**, *2*, 931.
- [7] P. Kambhampati, *Acc. Chem. Res.* **2011**, *44*, 1.
- [8] P. Kambhampati, *J. Phys. Chem. C* **2011**, *115*, 22089.
- [9] P. Tyagi, P. Kambhampati, *J. Chem. Phys.* **2011**, *134*, 094006.
- [10] F. Garcia-Santamaria, Y. F. Chen, J. Vela, R. D. Schaller, J. A. Hollingsworth, V. I. Klimov, *Nano Lett.* **2009**, *9*, 3482.
- [11] R. D. Schaller, M. A. Petruska, V. I. Klimov, *J. Phys. Chem. B* **2003**, *107*, 13765.
- [12] V. Sukhovatkin, S. Musikhin, I. Gorelikov, S. Cauchi, L. Bakueva, E. Kumacheva, E. H. Sargent, *Opt. Lett.* **2005**, *30*, 171.
- [13] E. A. Dias, J. I. Saari, P. Tyagi, P. Kambhampati, *J. Phys. Chem. C* **2012**, *116*, 5407.
- [14] A. G. Joly, W. Chen, D. E. McCready, J. O. Malm, J. O. Bovin, *Phys. Rev. B* **2005**, *71*, 165304.
- [15] T. C. He, R. Chen, W. W. Lin, F. Huang, H. D. Sun, *Appl. Phys. Lett.* **2011**, *99*, 081902.
- [16] G. S. He, P. P. Markowicz, T. C. Lin, P. N. Prasad, *Nature* **2002**, *415*, 767.

- [17] G. S. He, L. S. Tan, Q. Zheng, P. N. Prasad, *Chem. Rev.* **2008**, *108*, 1245.
- [18] E. E. Hoover, J. A. Squier, *Nat. Photonics* **2013**, *7*, 93.
- [19] N. G. Horton, K. Wang, D. Kobat, C. G. Clark, F. W. Wise, C. B. Schaffer, C. Xu, *Nat. Photonics* **2013**, *7*, 205.
- [20] T. C. He, D. Rajwar, L. Ma, Y. Wang, Z. B. Lim, A. C. Grimsdale, H. D. Sun, *Appl. Phys. Lett.* **2012**, *101*, 213302.
- [21] C. Zhang, F. Zhang, T. Zhu, A. Cheng, J. Xu, Q. Zhang, S. E. Mohney, R. H. Henderson, Y. A. Wang, *Opt. Lett.* **2008**, *33*, 2437.
- [22] J. J. Jasieniak, I. Fortunati, S. Gardin, R. Signorini, R. Bozio, A. Martucci, P. Mulvaney, *Adv. Mater.* **2008**, *20*, 69.
- [23] F. Todescato, I. Fortunati, S. Gardin, E. Garbin, E. Collini, R. Bozio, J. J. Jasieniak, G. Della Giustina, G. Brusatin, S. Toffanin, R. Signorini, *Adv. Funct. Mater.* **2012**, *22*, 337.
- [24] R. G. Xie, U. Kolb, J. X. Li, T. Basche, A. Mews, *J. Am. Chem. Soc.* **2005**, *127*, 7480.
- [25] E. A. Dias, S. L. Sewall, P. Kambhampati, *J. Phys. Chem. C* **2007**, *111*, 708.
- [26] F. Garcia-Santamaria, S. Brovelli, R. Viswanatha, J. A. Hollingsworth, H. Htoon, S. A. Crooker, V. I. Klimov, *Nano Lett.* **2011**, *11*, 687.
- [27] B.-H. Zhu, H.-C. Zhang, Z.-Y. Zhang, Y.-P. Cui, J.-Y. Zhang, *Appl. Phys. Lett.* **2011**, *99*, 231903.
- [28] G. Morello, F. Della Sala, L. Carbone, L. Manna, G. Maruccio, R. Cingolani, M. De Giorgi, *Phys. Rev. B* **2008**, *78*, 195313.
- [29] C. L. Gan, M. Xiao, D. Battaglia, N. Pradhan, X. G. Peng, *Appl. Phys. Lett.* **2007**, *91*, 201103.
- [30] G. C. Xing, S. Chakraborty, K. L. Chou, N. Mishra, C. H. A. Huan, Y. Chan, T. C. Sum, *Appl. Phys. Lett.* **2010**, *97*, 061112.
- [31] J. Lim, S. Jun, E. Jang, H. Baik, H. Kim, J. Cho, *Adv. Mater.* **2007**, *19*, 1927.
- [32] M. Sheikbaha, A. A. Said, T. H. Wei, D. J. Hagan, E. W. Vanstryland, *IEEE J. Quantum Electron.* **1990**, *26*, 760.
- [33] Y. Wang, X. Yang, T. C. He, Y. Gao, H. V. Demir, X. W. Sun, H. D. Sun, *Appl. Phys. Lett.* **2013**, *102*, 021917.
- [34] R. L. Sutherland, *Handbook of Nonlinear Optics*, 2nd Ed., Marcel Dekker, New York **2003**.
- [35] G. S. He, K. T. Yong, Q. D. Zheng, Y. Sahoo, A. Baev, A. I. Ryasnyanskiy, P. N. Prasad, *Opt. Express* **2007**, *15*, 12818.
- [36] J. W. M. Chon, M. Gu, C. Bullen, P. Mulvaney, *Appl. Phys. Lett.* **2004**, *84*, 4472.
- [37] J. He, W. Ji, J. Mi, Y. G. Zheng, J. Y. Ying, *Appl. Phys. Lett.* **2006**, *88*, 181114.
- [38] W. W. Yu, L. H. Qu, W. Z. Guo, X. G. Peng, *Chem. Mater.* **2003**, *15*, 2854.
- [39] V. I. Klimov, S. A. Ivanov, J. Nanda, M. Achermann, I. Bezel, J. A. McGuire, A. Piryatinski, *Nature* **2007**, *447*, 441.
- [40] X. Y. Wang, X. F. Ren, K. Kahen, M. A. Hahn, M. Rajeswaran, S. Maccagnano-Zacher, J. Silcox, G. E. Cragg, A. L. Efron, T. D. Krauss, *Nature* **2009**, *459*, 686.
- [41] R. R. Cooney, S. L. Sewall, D. M. Sagar, P. Kambhampati, *Phys. Rev. Lett.* **2009**, *102*.
- [42] R. R. Cooney, S. L. Sewall, D. M. Sagar, P. Kambhampati, *J. Chem. Phys.* **2009**, *131*.
- [43] D. S. Wiersma, *Nat. Phys.* **2008**, *4*, 359.
- [44] H. Cao, *Waves in Random Media* **2003**, *13*, R1.
- [45] H. Cao, Y. G. Zhao, S. T. Ho, E. W. Seelig, Q. H. Wang, R. P. H. Chang, *Phys. Rev. Lett.* **1999**, *82*, 2278.
- [46] L. Cerdan, E. Enciso, V. Martin, J. Banuelos, I. Lopez-Arbeloa, A. Costela, I. Garcia-Moreno, *Nat. Photonics* **2012**, *6*, 621.
- [47] A. Tulek, R. C. Polson, Z. V. Vardeny, *Nat. Phys.* **2010**, *6*, 303.
- [48] H. Cao, J. Y. Xu, D. Z. Zhang, S. H. Chang, S. T. Ho, E. W. Seelig, X. Liu, R. P. H. Chang, *Phys. Rev. Lett.* **2000**, *84*, 5584.
- [49] R. Chen, Q. L. Ye, T. C. He, V. D. Ta, Y. J. Ying, Y. Y. Tay, T. Wu, H. D. Sun, *Nano Lett.* **2013**, *13*, 734.
- [50] H. C. Hsu, C. Y. Wu, W. F. Hsieh, *J. Appl. Phys.* **2005**, *97*, 064315.
- [51] B. Liu, R. Chen, X. L. Xu, D. H. Li, Y. Y. Zhao, Z. X. Shen, Q. H. Xiong, H. D. Sun, *J. Phys. Chem. C* **2011**, *115*, 12826.
- [52] R. C. Polson, A. Chipouline, Z. V. Vardeny, *Adv. Mater.* **2001**, *13*, 760.
- [53] W. K. Bae, K. Char, H. Hur, S. Lee, *Chem. Mater.* **2008**, *20*, 531.